ADVANCES IN ATMOSPHERIC SCIENCES, VOL. 25, NO. 3, 2008, 481–488

Improvement of Surface Albedo Simulations over Arid Regions

BAO Yan*[1,2,3] (鲍 艳), LÜ Shihua[1] (吕世华), ZHANG Yu[1] (张 宇),
MENG Xianhong[1] (孟宪红), and YANG Shengpeng[1] (杨胜朋)

[1] *Cold and Arid Regions Environmental and Engineering Research Institute, Chinese Academy of Sciences, Lanzhou* 730000

[2] *Institute of Desert Meteorology, China Meteorological Administration, Ürümqi* 830002

[3] *Institute of Plateau Meteorology, China Meteorological Administration, Chengdu* 610000

(Received 30 April 2007; revised 31 October 2007)

ABSTRACT

To improve the simulation of the surface radiation budget and related thermal processes in arid regions, three sophisticated surface albedo schemes designed for such regions were incorporated into the Biosphere-Atmosphere Transfer Scheme (BATS). Two of these schemes are functions of the solar zenith angle (SZA), where the first one has one adjustable parameter defined as SZA1 scheme, and the second one has two empirical parameters defined as SZA2 scheme. The third albedo scheme is a function of solar angle and soil water that were developed based on arid-region observations from the Dunhuang field experiment (DHEX) (defined as DH scheme). We evaluated the performance of the original and newly-incorporated albedo schemes within BATS using the *in-situ* data from the Oasis System Energy and Water Cycle Field Experiment that was carried out in JinTa, Gansu arid area (JTEX). The results indicate that a control run by the original version of the BATS generates a constant albedo, while the SZA1 and SZA2 schemes basically can reproduce the observed diurnal cycle of surface albedo, although these two schemes still underestimate the albedo when SZA is high in the early morning and late afternoon, and overestimate it when SZA is low during noontime. The SZA2 scheme has a better overall performance than the SZA1 scheme. In addition, BATS with the DH scheme slightly improves the albedo simulation in magnitude as compared to that from the control run, but a diurnal cycle of albedo is not produced by this scheme. The SZA1 and SZA2 schemes significantly increase the surface absorbed solar radiation by nearly 70 W m^{-2}, which further raises the ground temperature by 6 K and the sensible heat flux by 35 W m^{-2}. The increased solar radiation, heat flux, and temperature are more consistent with the observations that those from the control run. However, a significant improvement in these three variables is not found in BATS with the DH scheme due to the neglect of the diurnal cycle of albedo. Further analysis indicates that during cloudy days the solar radiation simulations of BATS with these three schemes are not in a good agreement with the observations, which implies that a more realistic partitioning of diffuse and direct radiation is needed in future land surface process simulations.

Key words: arid region, bare soil, surface albedo, solar zenith angle (SZA), BATS

DOI: 10.1007/s00376-008-0481-y

1. Introduction

Surface albedo is very important for weather and climate modeling. It directly controls the partitioning of radiation energy over land surfaces, which, in turn, affects ecosystem physical, physiological, and biogeochemical processes such as surface energy balance, evaportranspiration, photosynthesis, and respiration (Wang et al., 2001, 2002a,b). It has long been recognized that accurate surface albedo information is indispensable for weather forecasting and climate modeling.

The false description of surface albedo in numerical models may cause great deviations in calculations of surface radiation and surface fluxes exchange. Recent studies show that the previously assumed albedo for the boreal forest in winter, which is set as the National Centers for Environmental Prediction model (NCEP)

*Corresponding author: BAO Yan, byan@lzb.ac.cn

(Kalnay et al., 1996) and the European Centre for Medium-Range Weather Forecasts model (ECMWF Technical Attachment, 1993), can be more than five times higher than actual magnitudes, and simulations using such magnitudes underestimate daily winter temperatures over the boreal region by 10 K–15 K (Betts and Ball, 1997, Baldocchi et al., 2000). Using an energy balance climate model, Otterman et al. (1984) conclude that the lower albedo of high-latitude forests in winter increases surface temperature at 65°N by 5 K.

Gobi and desert are two of the most important surfaces in arid regions, which have the strong radiation heating effects due to their high surface albedos. In most land surface models (LSMs), surface albedo of bare soil are taken to be a function of soil color and soil moisture (Dickinson and Kenney, 1986), but are independent on the solar zenith angle (SZAs). However, both satellite data and *in-situ* data have convincingly shown the significant geographic variation of desert albedo (Tsvetsinskaya et al., 2002; Wang, 2004), and they can be directly used in LSMs to address the uniformity assumption above. Remote sensing data from the satellite and aircraft platforms as well as field measurements have also shown the anisotropy of bare soil surface, because soils have relatively opaque vertical structures that cause dark shadows (Kimes, 1983). For instance, Monteith and Szeice (1961) show that the measured bare soil albedo increases from 0.16 at 30° SZA to 0.19 at 70° SZA with a daily mean of 0.17, Idso et al. (1975) found the curves of albedo as a function of the SZA for wet and dry conditions are identical in shape on average.

In recent years, some research has been done to parameterize surface albedo with different observations. For example, Paltridge and Partt (1981) summarizes the relationship between surface albedo and SZA, Wu and Zhong (1993) simply parameterize the surface albedo depending on SZA based on the observations of the "Heihe River Basin Field Experiment" (HEIFE), Zhang et al. (2002) obtained the relationship between surface albedo and sun angle with the observations of DHEX. Some remote sensing parameterizations about surface radiation over bare soil also have been done using satellite sensing data and observations from HEIFE, DHEX and JTEX (Ma et al., 2003, Meng et al., 2006). Wang et al. (2005) develop a one-parameter and a two-parameter schemes to calculate bare soil surface albedo on the base of Moderate Resolution Imaging Spectro-radiometer (MODIS) Bidirectional Reflectance Distribution Reflectance (BRDF) and albedo data over 30 deserts. This paper aims to evaluate these parameterization schemes in land surface models and improve the simulation of the radiation budget and surface thermal processes over bare soil.

2. Methodology

BATS is used in this research. In BATS, the albedo of bare soil is calculated by formula (1):

$$\alpha = \alpha_{\rm sat} + \Delta\alpha_g(S_{\rm sw}) \,, \tag{1}$$

where $\alpha_{\rm sat}$ is the albedo of a saturated soil, $S_{\rm sw}$ is the ratio of surface soil water content, and an increase of albedo due to dryness of surface soil within the wavelength $\lambda < 0.7$ μm can be calculated by formula (2):

$$\Delta\alpha_g(S_{\rm sw}) = 0.01(11 - 40S_{\rm sw}/Z_{\rm u}) > 0 \,, \tag{2}$$

where $Z_{\rm u}$ is the upper soil layer depth. This formula is chosen so that albedos range in a nonlinear fashion between the saturated and dry magnitudes. The magnitude of $S_{\rm sw}$ becomes very small ($\leqslant 0.025$ m) before and when the soil albedo shows a significant increase. Moisture is retained around the soil grains until 80% dryness occurs. The diffuse albedo is simply assumed to be synonymous with direct albedo, and soil albedos within $\lambda > 0.7$ μm are twice as much as those within $\lambda < 0.7$ μm.

In the research of Wang et al. (2005), direct albedo of bare soil normalized by its magnitude at 60° SZA can be adequately represented by a one-parameter formula (Briegleb et al., 1986) and a two-parameter formula (Ranson et al., 1991, Schaaf et al., 2002):

$$\alpha(\theta) = \alpha_r \cdot \frac{1+C}{1+2C^* \cos\theta} \,, \tag{3}$$

$$\alpha(\theta) = \alpha_r \cdot \{1 + B_1[g_1(\theta) - g_1(60°)] + B_2[g_2(\theta) - g_2(60°)]\} \,. \tag{4}$$

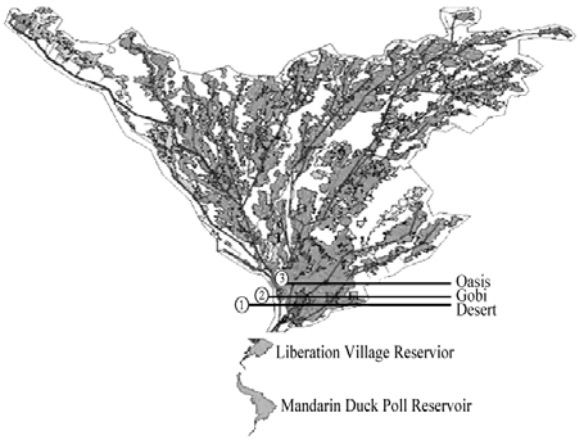

Fig. 1. Location of Jinta Gobi and Desert site.

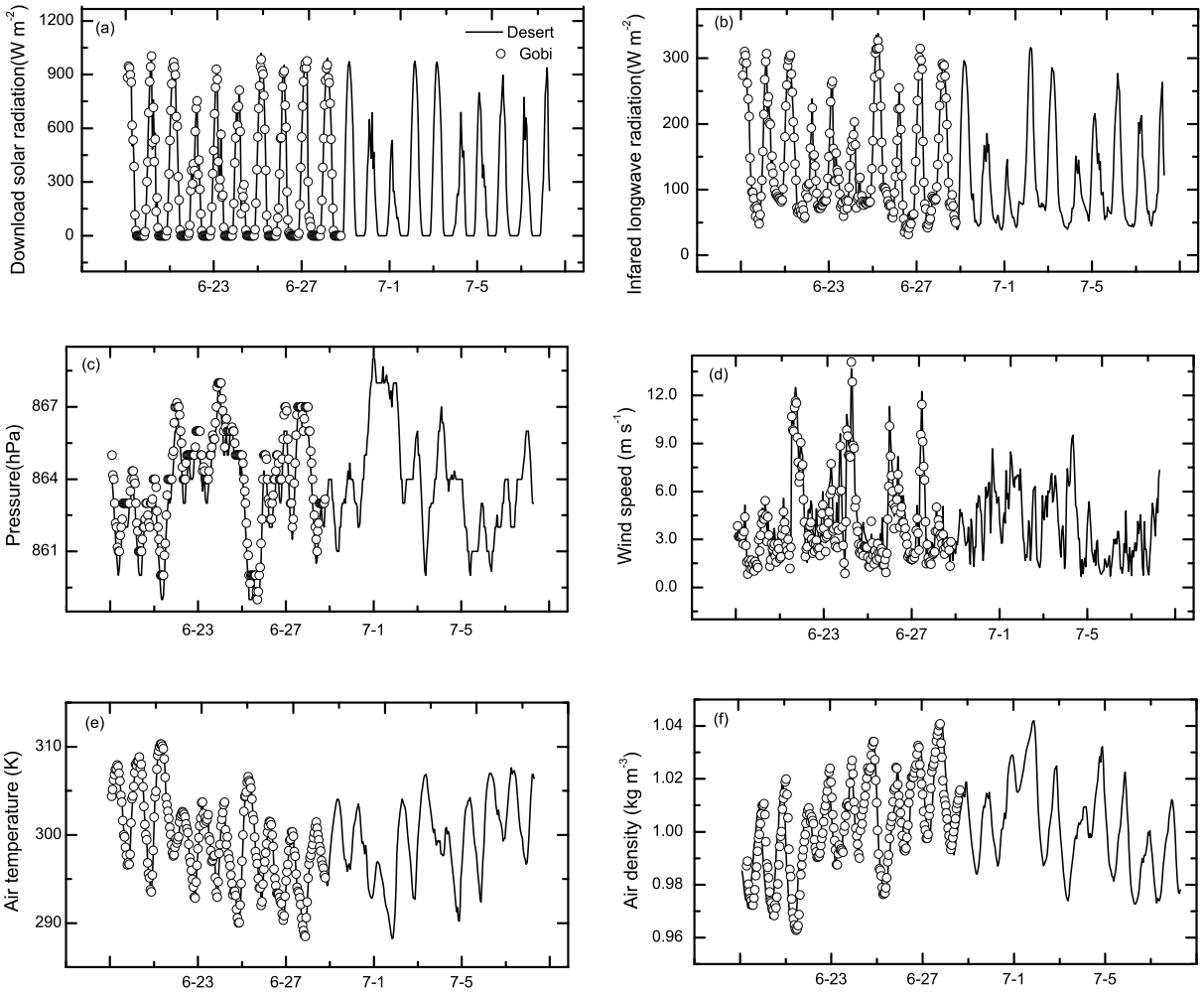

Fig. 2. Atmospheric forcing data: (a) Downward solar radiation (W m^{-2}); (b) infrared long-wave radiation (W m^{-2}); (c) pressure (hPa); (d) wind speed (m s^{-1}); (e) air temperature (K); (f) air density (kg m^{-3}).

Table 1. Location information of Gobi and Desert site and underlying surface characteristics.

Jinta Site	Location	Underlying surface characteristics
Gobi	39°58.535′N, 98°51.518′E	sand and gravel (sand 93.5%)

With the analyses of MODIS/BRDF and the albedo data over 30 deserts, the empirical parameters C, B_1, and B_2 are set as 0.15, 0.346 and 0.063. In Eqs. (3) and (4), α_r is the albedo at 60° SZA and its magnitude depends on season and location; θ is solar zenith angle. The g_1 functions and g_2 are from the algorithm (Schaaf et al., 2002):

$$\begin{cases} g_1(\theta) = -0.007574 - 0.070987\theta^2 + 0.307588\theta^3 \\ g_2(\theta) = -1.284909 - 0.166314\theta^2 + 0.041840\theta^3 \end{cases} \quad (5)$$

In Eq. (4), the parameters B_1 and B_2 are the average of the ratio of the volumetric and geometric parameters in the MODIS algorithm over α_r for 30 pixels, respectively. Diffuse albedo is the integral of all SZAs with the weigh of $\cos\theta$.

Zhang et al. (2002) obtain the formula by fitting the measured soil albedo and the relative factors using *in situ* data of Dunhuang Gobi from August 2000 to September 2001:

$$\alpha = (1 - 0.0074 w_{\rm s})(0.20 + 0.090^{-0.01^* h_\theta}) \,, \quad (6)$$

where $w_{\rm s}$ is the water content at surface layer of soil, h_θ is solar elevation angle. This albedo is the mixture of a direct albedo and a diffuse one.

3. Data

We incorporate these schemes in BATS, which is forced by atmospheric observations at the Jinta Gobi and Desert (LÜ et al., 2005). Figure 1 and Table 1

Table 2. Measured albedos over Gobi and Desert surface.

Field Experiment	Station site	Location	Altitude (m)	Surface type	Albedo
HEIFE	Huayin	39°09′N, 100°05′E	1454	Gobi	0.248±0.011 (Wu and Zhong, 1993)
	Huayin	39°26′N, 100°12′E	1378	Desert	0.225±0.013 (Wu and Zhong, 1993)
DHEX	Dunhuang	40°10′N, 94°31′E	1150	Gobi	0.255±0.021 (Zhang et al., 2002)
JTEX	Jinta	39°58′N, 98°52′E	1280	Gobi	0.249

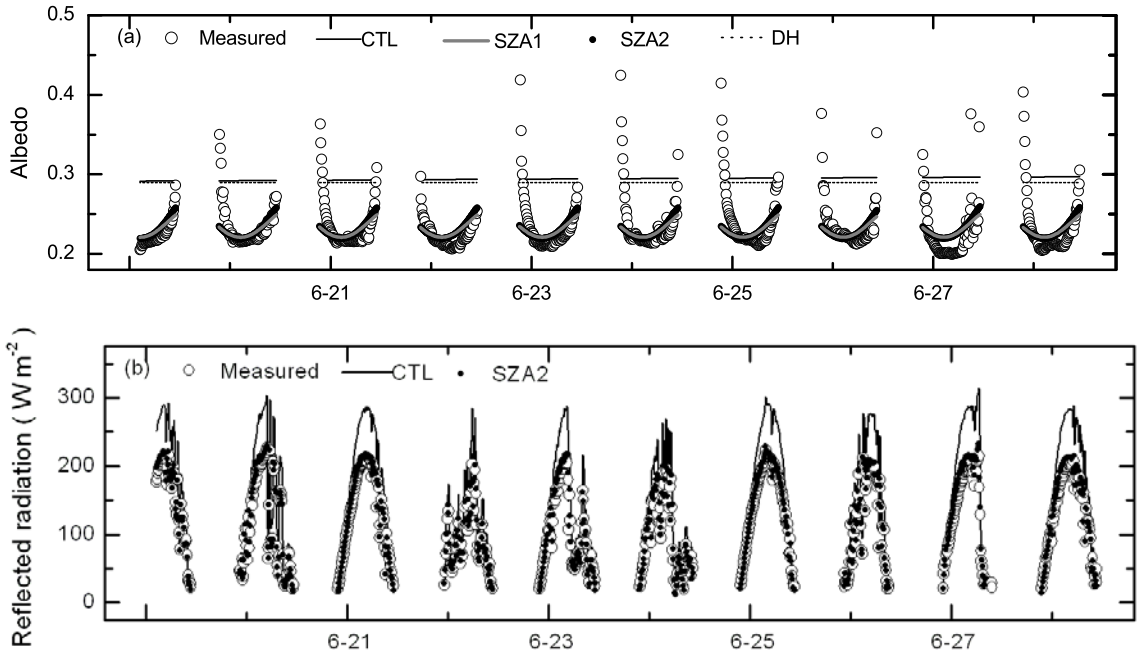

Fig. 3. Diurnal variation of surface albedo and reflected radiation over Gobi surface (a) surface albedo (b) reflected radiation (W m^{-2}).

show the information about locations and surface conditions, and Fig. 2 gives the atmospheric forcing information. We run the model independently from 19 June to 28 June at the Gobi site and from 19 June to 8 July at the Desert Site according to the observations. Before performing the simulations, some parameter calibrations have been done in the original BATS simulation (CTL experiment) based on the land parameters measured in DHEX, including surface roughness length, soil wetness factor, and thermal exchange coefficient, which significantly improve the performance of surface thermal heat flux but have little effect on surface radiation modeling in the former experiments.

4. Results

4.1 *Albedo and reflected solar radiation*

At different wavelengths, the model simulates surface albedo for direct and diffuse radiation. However, since only the total shortwave radiation (TSW) is measured in the Jinta site, we focus on the comparison of TSW results in this section.

The diurnal variations of surface albedos have different patterns in different weather conditions (Fig. 3a). On clear days (e.g., 21 June), albedos have a pattern close to "U"-shape with a minimum at noon, which has also been reported in other research (e.g., Zhang et al., 2002). On overcast days (e.g., 22 June), albedos show small diurnal variation because the diffuse radiations with limited scope of angular distributions of SZAs dominate in TSW in these weather conditions (e.g., 23–27 June), and albedos change significantly when the ratio of direct radiation versus diffuse radiation changes dramatically with the variation of cloud coverage. To conclude, albedos in clear weather conditions are slightly higher than those in cloudy and overcast weather conditions. Similar albedo characteristics are also measured at the desert site (figure

Table 3. Deviation analysis of reflected solar radiation over Gobi.

Reflected solar radiation	CTL	SZA1	SZA2	DH
Standard errors (W m^{-2})	75.2	8.6	8.4	68.4
Relative errors (%)	34	5.6	5.2	32.5

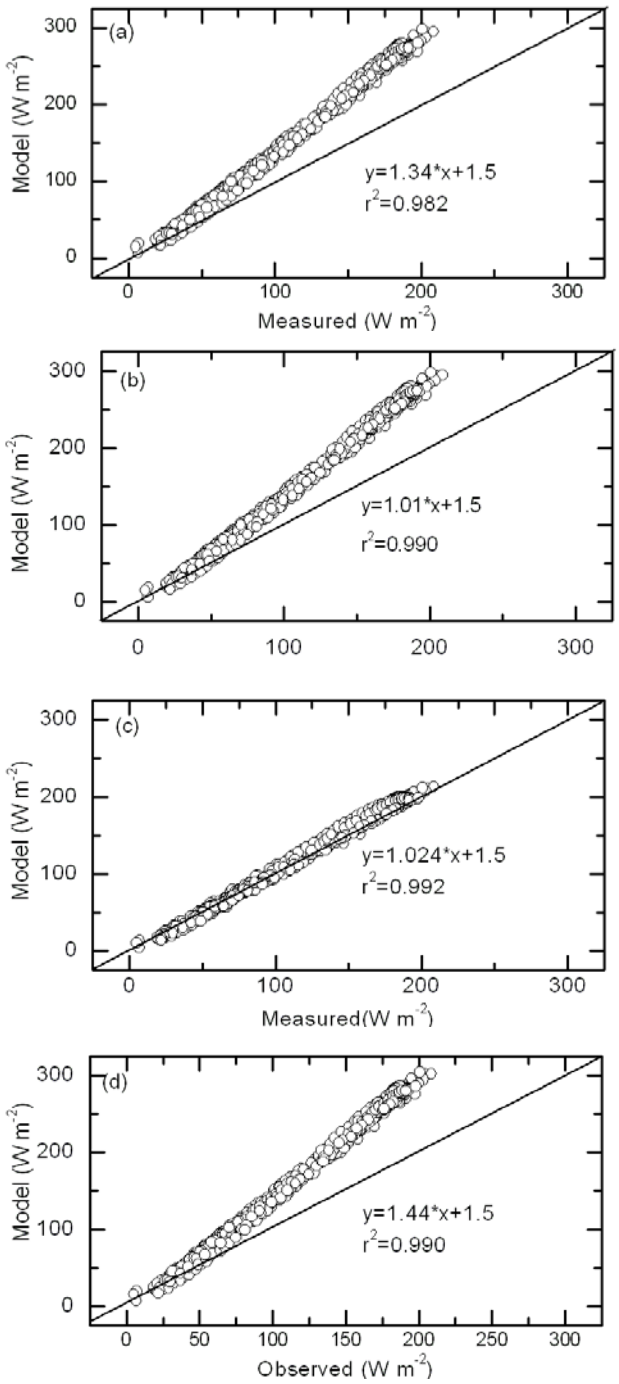

Fig. 4. Regression analysis of measured and simulated surface reflected solar radiation over Gobi and Desert site. (a) Simulations of CTL experiment (b) SZA1 method (c) SZA2 method (d) DH method.

omitted).

However, it is worth noting that some extremely high albedo magnitudes are measured in the early morning over Gobi and Desert. This diurnal asymmetry of surface albedo has also been observed in grassland ecosystems (Minnis et al., 1997; Song, 1998), possibly caused by dew on the canopy in early morning. In our research, the variations of soil moisture and SZA are the most important two factors that affect the surface albedo, but they can't interpret the very high magnitudes measured in the early morning, which possibly result from the measured deviation of diffuse radiation.

In the CTL experiment, the simulated albedo is almost constant, with magnitudes 0.29 (Fig. 3a), which are much higher than those measured at the Gobi site in Huain Gobi and Dunhuang Gobi, which are located at a similar latitude to Jinta Site (Table 2). Albedos simulated from the SZA1 method and from the SZA2 method have good agreement with the measurements, except for the low albedo in the early morning or in the late afternoon in the high SZA and the higher albedo at noon time at the lower SZA, ranging from 0.2 to 0.3 over the Gobi. There are very minor differences between the results of the SZA1 method and that of the SZA2 method, except for the larger magnitude in the early morning and in the late afternoon simulated in method SZA2. This indicates that the SZA2 method is more sensitive to the larger SZA than SZA1 method. DH method simulates the smaller diurnal variation and higher values just as the CTL experiment. We also found that the four methods perform better on clear days than on cloudy and overcast days due to the radiation effect of clouds since the diffuse radiation dominates in total radiation under these weather conditions.

Based on the simulated albedo, we calculate the relevant reflected radiation (Fig. 3b). The simulated reflected radiation has good agreement with the observations during the simulation periods, except that the model fails to capture the lower albedo (the reflected radiation at very higher SZA (>70°) has not been showed in the study) during noon time. Due to this deviation, the standard deviations are, respectively, 75.2 W m^{-2} and 68.4 W m^{-2} and about 30% overestimate in CTL and DH method, while standard deviation are 8.4 W m^{-2} and 8.6 W m^{-2}, or 5.2% and 5.6% overestimation of SZA2 method and SZA1

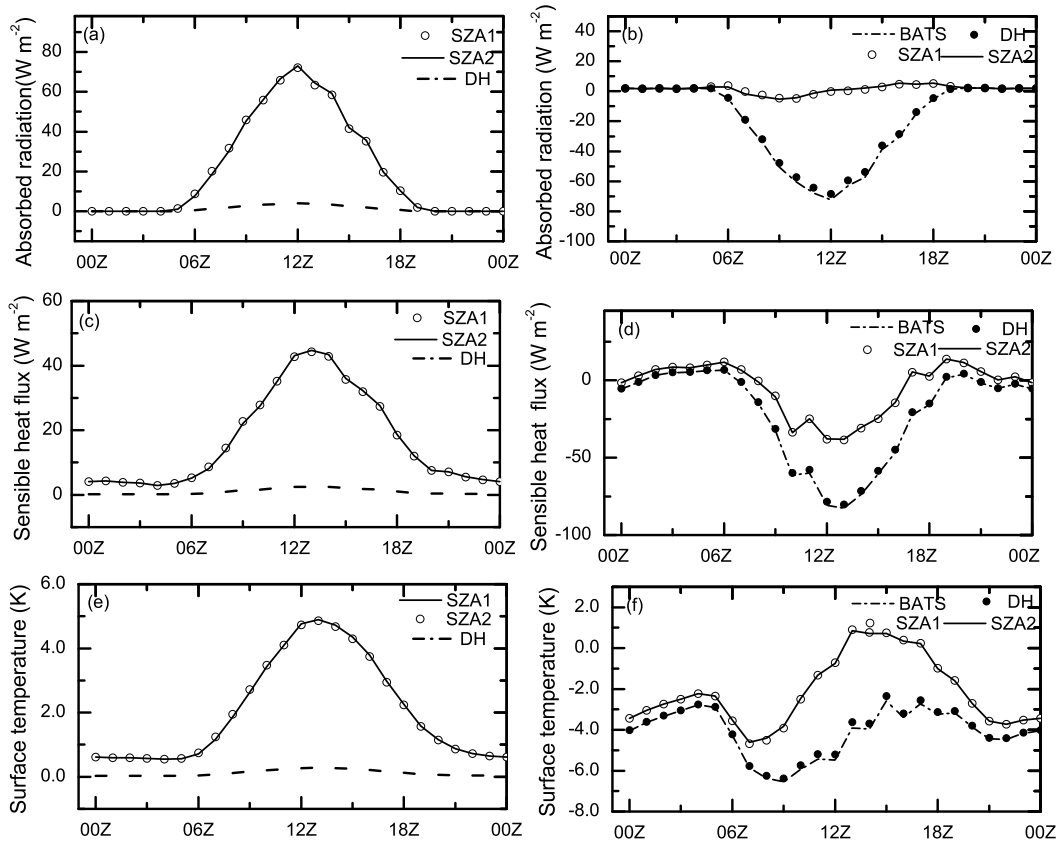

Fig. 5. Differences of diurnal variations between simulations of methods B, SZA2, DH and CTL experiment and the observations. Panels on the left are the differences between simulations and CTL experiment (simulations−CTL), on the right are the differences between simulations and observations (simulations–observations). (a) and (b) are surface absorbed solar radiation (W m^{-2}), (c) and (d) are for surface sensible heat flux (W m^{-2}), (e) and (f) are ground temperature (K).

Table 4. Difference between simulated absorbed solar radiation, sensible flux, surface temperature of SZA1,SZA2 and DH scheme with CTL (-CTL) or with observations(-observations).

	Surface absorbed radiation (W m^{-2})		Sensible heat flux (W m^{-2})		Ground temperature (K)	
	CTL	Observed	CTL	Observed	CTL	Observed
CTL		−67.75		−74.52		−4.93
SZA1	67.16	−0.59	40.76	−33.76	4.56	+0.37
SZA2	67.97	0.22	40.95	−33.56	4.58	+0.35
DH	3.75	−64.00	2.33	−72.19	0.26	−4.67

method over Gobi (Table 3). The simulations over the desert have the similar conclusions (figure omitted)

Figure 4 shows the overall regression relationship between the measured and simulated reflected radiation for the first 10 days during the simulating period (19–28 June) over the Gobi. Results show that the simulated reflected radiation is much higher than the measurements, especially when the reflected radiation is more than 100 W m^{-2}. The simulations of the SZA2 method and the SZA1 method slightly overestimate the measured reflected radiation resulting from the higher albedo of the SZA2 method and the SZA1 method at solar noon discussed above (as shown by the deviation from the 1:1 line in Fig. 4).

4.2 *Simulation of surface thermal fluxes and ground temperature*

Figure 5a shows the overall deviations between the simulated and measured surface absorbed solar radiation over the Gobi and Desert during the simulating period. Compared with CTL experiment, the SZA1 method, the SZA2 method, and the DH method, re-

spectively, overestimate the absorbed solar radiation by 67.16 W m^{-2}, 67.97 W m^{-2} and 3.75 W m^{-2} at solar noon (Fig. 5a, Table 3). Since less solar radiation is incident at low sun angles, the higher albedos do not affect the simulations at sunrise and sunset. About 63% of the extra solar energy goes into an increase of sensible heat flux (Fig. 5c), while another 14% is transferred into the soil (omitted). The remaining energy is primarily used to increase the ground temperature (Fig. 5e) and is emitted as long-wave radiation. Compared with the CTL experiment, the ground temperature at local solar noon is higher by 4.56 K, 4.58 K, and 0.23 K, respectively, of the SZA1 method, the SZA2 method, and the DH method.

There are systematic minus deviations in ground temperature simulations in the CTL simulation due to the low absorbed solar radiation. Simulated albedos from the SZA1 method, the SZA2 method, and the DH method significantly improve the minus bias in surface fluxes. Compared to the measurements, the deviation of absorbed solar radiation during solar noon is respectively reduced from -67.75 W m^{-2} to -0.59 W m^{-2}, $+0.22$ W m^{-2} and -64 W m^{-2} in the SZA1 method, the SZA2 method, and the DH method (Fig. 5b, 5d, 5e), which directly resulted in the decrease of sensible heat flux with almost one half in the SZA1 method and the SZA2 method, or 2 W m^{-2} in the DH method. The minus deviation of ground temperature -5 K reduced to $+0.37$ K, $+0.35$ K, and -4.67 K in the SZA1 method, the SZA2 method, and the DH method.

5. Conclusions and discussion

We carried out experiments to evaluate some surface albedo schemes over bare soil and improve the modeling of surface radiation and thermal processes in arid regions. These schemes include Wang et al.'s two schemes depending on SZA (Wang et al., 2005) and Zhang's one scheme (Zhang et al., 2002) depending on SZA and Zhang's one scheme depending on solar angle and soil water based on observations of DHEX. The major conclusions are:

Some measured surface albedos over Gobi and Desert are presented in this paper, and some extremely high albedo magnitudes are measured in early morning over Gobi and Desert, which possibly have something to do with the measured deviations.

BATS simulates the high and almost constant albedo over Gobi and Desert, which cause high simulated reflected radiation and the minus deviation of surface sensible heat flux, as well as the ground temperature. The SZA2 method and the SZA1 method perform well in diurnal variations except that they underestimate the albedos in high SZAs in the morning and in the late afternoon, and they overestimate the albedos at lower SZA during noon time, which result in slight overestimations in reflected solar radiation. These improvements greatly reduce the minus deviation of surface absorbed radiation by 60 W m^{-2} and sensible heat flux by one half, as well as the ground temperature bias from -5 K to less than $+1$ K during noon time. The DH method provides little improvement in surface fluxes and ground temperature since it simulates too high an albedo at noon and it is not as sensitive to SZA.

Generally, simulated albedos on cloudy days and overcast days are not as good as that on clear days due to the diffuse radiation effect of cloud, which indicates the effects of clouds must be considered in future LSMs. Further work include comprehensively evaluating its impact on coupled climate and improve the performance of regional climate in arid regions.

Acknowledgements. The authors wish to thank Dr. Zhou Liming and Dr. Jin Jiming and Dr. Yang Wen for providing constructive instructions. This research is supported by the Key Directional Program of Knowledge Innovative Project of Chinese Academy of Sciences under grant KZCX2-YW-220 and by Institute of Desert Meteorology, Ürümqi, China Meteorological Administration (CMA) open foundation project under Grant SQJ200708 and by Institute of Arid Meteorology, Lanzhou, China Meteorological Administration (CMA) open foundation project under Grant IAM200608.

REFERENCES

Baldocchi, D., F. M. Kelliher, T. A. Black, and P. G. Jarvis, 2000: Climate and vegetation controls on boreal zone energy exchange. *Global Change Biology*, **6**(Suppl), 69–83.

Betts, A. K., and J. H. Ball, 1997: Albedo over the boreal forest. *J. Geophys. Res.*, **102**(D24), 28901–28910.

Briegleb, B. P., P. Minnis, V. Ramanmthan, and E. Harrison, 1986: Comparison of regional clear sky albedos inferred from satellite observations and model calculations. *Journal of Climate and Applied Meteorology*, **25**, 214–226.

Dickinson, R. E., and P. J. Kenney, 1986: Biosphere atmosphere transfer scheme (BATS) for the NCAR Community Climate Model. NCAR Technical Note NCAR/TN-275+STR, Boulder, Colorado, 69pp.

ECMWF Technical Attachment, 1993: The description of the ECMWF/WCRP Level III—A global atmospheric data archive. European Centre for Medium Range Weather Forecasts, Reading, England.

Idso, S. B., R. D. Jackson, R. J. Reginato, B. A. Kimbal, and F. S. Nakayama, 1975: The dependence of bare soil albedo on soil water content. *J Appl. Meteor.*,

14, 109–113.

Kalnay, E., and Coauthors, 1996: The NCEP/NCAR 40-year reanalysis project. *Bull. Amer. Meteor. Soc.*, **77**, 437–471.

Kimes, D. S., 1983: Dynamics of directional reflectance factor distributions for vegetation canopies. *Appl. Opt.*, **22**, 1364–1372.

LÜ, S. H., L. Y. Shang, L. Liang, and S. Q. Luo, 2005: Desert and oasis circulation in Jinta. *Plateau Meteorology*, **27**, 111–118. (in Chinese)

Ma, Y. M., J. M. Wang, R. H. Huang, G. A. Wei, Massimo Menenti, Z. B. Su, Z. Y. Hu, F. Gao, and J. Wen, 2003: Remote sensing parameterization of land surface heat fluxes over arid and semi-arid areas. *Adv. Atmos. Sci.*, **20**(4), 530–539.

Meng, X. H., S. H. LÜ, and L. J. Wen, 2006: Surface net solar radiation and net radiation retrieval over Jinta Area of the Middle Reaches of the Heihe River by using satellite data. *Plateau Meteorology*, **227**(8), 748–753. (in Chinese)

Minnis, P., S. Mayor, W. L. Simth Jr., and D. F. Yong, 1997: Asymmetry in the diurnal variation of surface albedo. *IEEE Trans. Geosci. Remote Sens.*, **35**, 879–891.

Monteith, J., and G. Szeice, 1961: The radiation balance of bare soil and vegetation. *Quart. J. Roy. Meteor. Soc.*, **87**, 159–170.

Otterman, J., M.-D. Chou, and A. Arking, 1984: Effects of non-tropical forest cover on climate. *Journal of Climate and Applied Meteorology*, **23**, 762–767.

Paltridge, G. W., and C. M. R. Partt, 1981: *The Radiation Processes in Meteorology and Climatology.* Translated by Lu Daren, Huang Runheng, and Lin Hai. Science Press, Beijing, 84–87.

Ranson, K. J., J. R. Irons, and C. S. T Daughtry, 1991: Surface albedo from bidirectional reflectance. *Remote Sens. Environ.*, **35**, 201–211.

Schaaf, C. B., and Coauthors, 2002: First operational SZA2 albedo nadir reflectance products from MODIS. *Remote Sensing of Environment*, **83**, 135–148.

Song, J., 1998: Diurnal asymmetry in surface albedo. *Agricultural and Forest Meteorology*, **92**, 181–189.

Tsvetsinskaya, E. A., C. B. Schaaf, F. Gao, A. H. Strahler, R. E. Dickinson, X. Zeng, and W. Lucht, 2002: Relating MODIS-derived surface albedo to soils and rock types over Northern Africa and the Arabian Peninsula. *Geophys. Res. Lett.*, **29**, 1353, doi: 10.1029/2001GL014096.

Wang, S., R. F. Grant, D. L. Verseghy, and T. A. Black, 2001: Modeling plant carbon and nitrogen dynamics of a boreal aspen forest in CLASS-the Canadian Land Surface Scheme. *Ecological Modelling*, **142**, 135–142.

Wang, S., R. F. Grant, D. L. Verseghy, and T. A. Black, 2002a: Modeling carbon-coupled energy and water dynamics of a boreal aspen forest in a General Circulation Model Land Surface Scheme. *International Journal of Climatology*, **22**, 1249–1265.

Wang, S., R. F. Grant, D. L. Verseghy, and T. A. Black, 2002b: Modeling carbon dynamics of boreal forest ecosystems using the Candadian Land Surface Scheme. *Climatic Change*, **55**, 451–477.

Wang, Z., 2004: Using MODIS SZA2 and albedo data to evaluate global model land surface albedo. *Journal of Hydrometeorology*, **5**, 3–14.

Wang, Z., M. Barlage, X. Zeng, R. E. Dickinson, and C. B. Schaaf, 2005: The solar zenith angle dependence of desert albedo. *Geophys. Res. Lett.*, **32**, L05403, DOI:10. 1029/2004GL 021835.

Wu, A. S., and Q. Zhong, 1993: Relationships between global surface albedo and solar elevation angle for several underlying surfaces in the HEIFE experimental area. *Plateau Meteorology*, **12**, 147–155. (in Chinese)

Zhang, Q., X. Y. Cao, and G. A. Wei, 2002: Observation and study of some key parameters of land surface process of Gobi in arid region. *Adv. Atmos. Sci.*, **19**, 1–14.